DERIVATION OF APPROXIMATE VALUES BY RECOGNITION OF CIRCULAR TARGETS

Ingolf Hådem
University of Trondheim
Division of geodesy and photogrammetry
N-7034 Trondheim
Norway
Commission V

Summary

An algorithm is presented for digital recognition of projected circular targets situated within a window of a digital frame or digitized photo. Functions that the algorithm performs are: segmentation by thresholding, search by a simple operator to identify the image of the target, and digitally measuring its shape and its position in the window. The algorithm can be used for providing initial approximate values for: (a) a highly accurate point determination, (b) template matching, and (c) bundle adjustment.

A small practical experiment was performed using this algorithm on data acquired by first photographing a targeted close range test field, and then digitizing windows of the photos by the use of one CCD-camera of an analytical plotter (Kern). Figures for and comments on reliability and accuracy are given.

Introduction

In analytical close range photogrammetry, the derivation of initial approximate values for the bundle adjustment constitutes an important separate task which, if performed manually, might imply some additional time-consuming work (like preliminary measurement of camera rotations during the photographing). To make photogrammetry faster, automatic derivation of approximate values had been proposed. It should be ephasized that the equations, on which the bundle method is based, are of the polynomial type which cannot generally be solved by non-iterative techniques. However, particular methods for closed solution of redundant equations in the cases of re-section of single photos and relative orientation of stereo pairs have been developed (Killian and Meissel (1977), Hoffmann -Wellenhof (1978)). In the no-redundancy case, some search procedure or trial and error methods can be applied (Hådem (1984)).

In digital photogrammetry, the problem of obtaining approximate values might play a central role in certain operations. Some examples are:

- *iterative patch matching*; the central problem might be to find initial approximate location of conjugate patches, while approximation for the affine scaling and rotation are less problematic (Gruen and Baltavias (1987)).
- *digital measurement of pre-targeted points*; using a ring operator as described in Luhmann (1986), the derivation of approximate values is restricted to a coarse location of the projected target in the image; using template matching, approximations for all the affine transformation parameters are needed in principle.
- *bundle adjustment* on the basis of digitally measured image coordinates needs approximations for unknown parameters in the equations for the central perspective.

Approximate pixel gray values are also needed for matching operations.

The following discussion is focussed on the problem of deriving approximate values from a simple but fast digital recognition of projected circular targets. (A pattern of concentric circles is projected onto the image plane as a pattern of concentric ellipses). The digital recognition includes the detection and location of edges describing ellipses and digital measurement of the ellipse centre (x_c,y_c), the direction κ' of the major axis, and the sizes of the major and the minor semi-axes (a, b) of the ellipse (see fig. 1).

From evaluated ellipse parameters, initial values can be derived for: a) point determination by scale- and rotation-invariant operators, b) template matching, and c) bundle adjustment.

a) The use of *a scale- and rotation-invariant point determination* operator like that described by Luhmann (1986) requires only an initial location of the imaged target. If the target were to consist of a combination of circular and crossing features (the latter for the use of the above-mentioned operator, see fig. 4, c and d), the initial location could be based on recognizing ellipses and determining their common centre. The pattern of the crossing features should preferably consist of several intersection lines or edges designed in such a way that optimum intersection is achieved (thus, fig 5,b is more favourable than fig. 5,a). The combination of circular and crossing features might complicate the digital recognition.

b) Initial digital shape measurement of imaged circular targets might constitute a basis for deriving approximate values for a consequent *matching prodedure.* Template matching is an alternative to using rotation- and scale-invariant point determination operators in such cases like fig. 4, c and d, and is the appropriate method for recognizing numbers like fig. 5,c. It should, however, be noted that a digital point determination by matching an elliptical image with a circular template, needs approximate values for 5 geometric parameters (see Appendix D), while template matching for recognizing non-circular patterns needs approximate values for the 6 affinity parameters. Assuming that the target consists of both circular and non-circular features (e. g. fig. 5, c), these 6 values can be derived from measuring the ellipse parameters and an additional parameter α' determined by some additional feature, see fig. 7. (This derivation will not be further discussed).

c) Inital digital shape measurement as described above might constitute a basis for deriving approximate values for the camera orientation. Such values could be used for a consequent *bundle adjustment.* Such values could also be used for deriving initial values for the local affinity, for either matching the local image area with a template of the corresponding area in a plane object (see Appendix C, a), or matching the two local homologous areas that are images of the corresponding object area (see Appendix C, d). Two methods for deriving the orientation from ellipse recognition will be mentioned:

1) The most simple procedure might consist of the following operations:
- estimate the parameters of the outer ellipse for a sufficient number n of imaged targets,
- derive the scales $m_{i\ (i=1,..n)}$ of ellipse centres (radius r of outer target circle is given),
- derive bundle orientations and object point locations by solving linear equations.

These equations are given in Appendix B. If a targeted point has known object coordinates, equations (B4) expressing the co-linearity condition can be used; If this point is unknown and is imaged in a stereo pair, equations (B7) expressing the co-planarity condition can be used.

2) A more complex procedure for deriving approximate values of the outer orientation might be to use only one circular target with some additional non-circular feature. The outer orientation might refer to a local target system with its X,Y-plane equal to the target plane and its origin at the target centre. The additional object feature (e. g. point P, imaged as P', fig. 7) determines the direction of the X-axis. (If an absolute orientation in the global system is desired, the relation between the target system and the global system must be known). From measuring the 5 ellipse parameters and the above-mentioned additional parameter, the 6 outer orientation parameters can be determined. Using the rotations κ, ν and α defined in Ackermann and Schwidewsky (1976), p. 23, ν can be interpreted as the angle between the target plane and the image plane. In Appendix C, c approximate formulas are given, for determining κ, ν and the distance between the perspective center and the target plane on the basis of the ellipse parameters. It should be noticed that the use of relatively small elliptical images might give rather coarse values of the outer orientation.

The algorithm for recognition of circular targets has been programmed in FORTRAN 77 on a PDP 11/75. The program was first tested on simulated digital images of circular targets. Then a small experimental test was performed in a close-range environment. The acquisition of data was established by using a Hasselblad camera (MK 70, 45 mm) to obtain analog images of a simple test field with circular targets, and one CCD-camera of a Kern DSR 11 for grabbing digital frames of the analog images. From this experiment conclusions about the accuracy and reliability of the algorithm will be drawn.

The algorithm

It will be assumed that the pattern of a circular target of the type shown in fig. 4 a,b is projected somewhere within a window which is represented by a matrix of gray level values:

$$\mathbf{A}_{IJ}.$$

Thus, the task of the algorithm is:

- to search and identify the pattern of the projected target in the image, on the basis of a priori knowledge of the geometrical and radiometrical properties of the object target,
- to estimate on the basis of located points on the edges defining the concentric ellipses:
  - centre (x_c, y_c) of the concentric ellipses,
  - semi-axes *a* and *b* of the outer ellipse.
  - direction κ' of the major axis

(The ellipse parameters are defined in fig. 1). The different steps are:

Step 1. The digital image **A** is converted into a binary image by thresholding, thereby getting gray level segments the borders of which describe concentric ellipses, fig. 3. The two new gray levels are denoted by:

$$g_{\text{bright}},\ g_{\text{dark}}$$

Step 2. A 1-D search by a simple filter operator is performed on the rows of A, one row at a time, for detecting and locating edges between the segments on the basis of the following similarity criteria:

- derived signs of the gradients are in accordance with a priori specifications.
- the estimated relation between the mutual distances between the edges, agrees with a priori spesifications.

The criterion for detection of an edge might be as simple as:

$$|g_{ij} - g_{i+1,\,j}| = g_{\text{bright}} - g_{\text{dark}}$$

and the edge location is then:

$$x = (i + 0.5) \cdot \text{pixelsize}, \quad y = j \cdot \text{pixelsize}$$

Step 3. The midpoint of the chords defined by the located edge points is detemined for each cross-section, and a diameter line is adjusted to the midpoints (line "Dia_1" in fig. 2).

Step 4. The procedure of step 2 is now applied to columns of A, and the procedure of step 3 gives a second diameter line (line "Dia_2" in fig. 2).

Step 5. The centre (x_c,y_c) of the ellpses is determined as the point of intersection between the two diameters.

Step 6. The direction κ' of of the major axis is computed by formula (A8), see Appendix A.

Step 7. A search alongside a re-sampled intensity gray-value vector through the centre (x_c,y_c) in direction κ' recognizes and locates the end points of the major axis of the outer ellipse, thus determining the semi-major axis *a* of the outer ellipse.

Step 8. A similar search along the minor axis determines the semi-minor axis *b*.

Remarks:

1. A simpler algorithm for recognizing the ellipse pattern would have been to search in x- (or y-) direction, to identify and locate a sufficient number of edge points for the determination of the shape parameters from the well-known ellipse equation. However, because only the pattern of edges within a cross section through the central part of the ellipse pattern can satisfy the similarity criteria, this simplification would have given an unfavourable distribution of edge points as the basis for the derivation of the parameters, see fig. 2.

2. An important practical question is how many concentric circles should the target most favourably be. The similarity criteria (see step 2 above) more effectively prevent misinterpretation when the number of concentric circles is large. On the other hand, this diminishes the size of the central part of the target to be hit by the searching, complicates the digital recognition and increases the probability that some circle, particularly the smaller (inner) circle, does not image sufficiently well. Such an insufficient imaging will most probably happen when the image of the target is small (in terms of pixels), and also when *b/a* is small.

3. The threshold level T is interactively determined as follows:
   - an initial value T_0 is computed as

     $$T_0 = k_1 g_{max} + k_2 g_{min}; \quad k_1+k_2=1$$

     where

     g_{max}, g_{min}: maximum, minimum value respectively, of

     $g'_{ij} = 0.25(g_{ij}+g_{i, j+1}+g_{i+1, j}+g_{i+1, j+1}), \quad i=1,2..(I-1); \quad j=1,2..(J-1)$

     k_1, k_2: a priori specified values
   - a segmentation is executed with $T=T_0$, and the result is shown on the screen for judgement
   - a new adjusted T is manually introduced
   - and so on.

4. Compared with such highly accurate (but also more complex) edge determination techniques described by e. g. Mikhail (1979), the technique of thresholding might introduce a significant common scale error in the estimation of *a* and *b*. This is particularly true when using one singular threshold level T for extracting all ellipses within an imaged target pattern, because significantly different optimal thresholds might be valid for the various ellipses (see fig. 3). (For further study on edge extraction and border determination by means of segmentation, see Gonzales and Wintz (1977), §7.1.1.1).

5. A more accurate and reliable (but more complicated) procedure for evaluating *a* and *b*, is obtained by extending the procedure above by the following additional steps:

   Step 9. Considering a system (x′,y′) with x′-axis parallel to the large ellipse axis (see (A2)), a search is performed along several intersecting lines in the x′-direction, for $y'=y'_i$ (i=1,..), each intersection line i giving two intersection points $(x'_1,y')_i$ and $(x'_2,y')_i$ on the ellipse. From each such point pair and the preliminary evaluated $b = b_0$ from step 8, one evaluation a_i of the semi-major axis is obtained from :

   $$a_i=\sqrt{b_0^2\Delta x'^2_i/(b_0^2-y'^2_i)}, \quad \Delta x'_i=0.5(x'_2-x'_1)_i$$

   A final value of *a* is obtained as an average of the individual evaluations (including the evaluation from *Step 7*):

   $$a_{final} = \Sigma a_i \,/\, \text{number of evaluations}$$

   Step 10. By a similar procedure, on the basis of searching along intersecting lines in the y′-direction (i. e. the direction of the minor axis), a final value of *b* is obtained.

6. A final least square adjustment with differentiated ellipse equations (derived from the formulas in Appendix A) with the coordinates of the located ellipse points as "observations" and with the above evaluated ellipse parameters as initial approximations, would give a more optimal, but also a more complex estimation of unknown parameters, with a better evaluation of the accuracy and reliability of the result.

7. *Noise removal* of the segmented image is most simply established by the operator:

   If $g_{ij} = g_{bright}$ and $S = 8\, g_{dark}$, then $g_{ij} = g_{dark}$

   if $g_{ij} = g_{dark}$ and $S = 8\, g_{bright}$, then $g_{ij} = g_{bright}$

   where

   $S = \Sigma g_{i+k,j+l}$, Σ for: k,l = -1,0,1; exept k,l = 0,0

A practical experiment

In order to access the described algorithm, a small practical experiment was undertaken in a close range environment at the Royal Institute of Technology, Stockholm.

A test range of 26 circular targets (20 of which were lying on tables) were photographed from different directions with the use of a Hasselblad camera MK 70, 45 mm. The targets showed three concentric circles defined by edges between dark and bright aeras (fig. 4,a,b). The area between the middle and the outer circles was either dark or bright (referred to as dark and bright rings). One photo (fig. 9) was selected as the basis for the digital measurement with a Kern DSR 11. The two most remote targets (7 and 8 in fig. 9) with their planes nearly parallel to image plane at the moment of exposure, were projected nearly circularly onto the image. The projections of the other targets were pronounced ellipses. On the basis of the digital measurements, one tried, for each projected target, to estimate the parameters of the outer ellipse: the centre (x_c,y_c), the semi axes (a,b) and the orientation (κ').

Reference data for evaluating accuracy and reliability of the digital estimation were established by ordinary analytical photogrammetry. First a bundle adjustment was carried out on the basis of: (a) measuring image coordinates (analogly with the Kern DSR 11), (b) measuring distances between some targets, and (c) constraining Z=constant for the targets lying on the tables (using an object system X,Y,Z with X,Y-axes lying in the table plane). Then reference values of a, b, and κ' were computed from triangulated camera orientation and measured ellipse centres (by formulas derived in Appendix C,a,b). No such reference values of a, b, and κ' were obtained for targets not lying on the tables.

Thus, the procedure for the analog and digital measurement with the Kern was:

- the analog image was inserted in the Kern instrument, and the fiducial marks were measured (analogly) in order to operate in the fiducial system.
- the measuring mark was centred manually on the imaged target.
- a frame was grabbed and a window (40 · 40 pixels, pixelsize = 15μ) containing the imaged target was stored on file, together with the coordinates of the centred measuring mark, as input to the program for deriving (on line) the digitally measured coordinates and their deviations from corresponding measuring mark coordinates.

All the 10 steps of the algorithm were applied. The re-sampling needed for the steps 7,.. 10 used the simple "nearest neighbour" interpolation. Fig. 6 shows an example of segmentation.

Reliability:

The following failures (gross errors) occurred:

- One bright target (10, fig. 9) could not be digitally measured as the contrast was too small
- Two targets showed relatively large deviations between manually and digitally derived image coordinates (see table 1, note 3). The imagings of these targets were disturbed by considerable noise. It can, however, be assumed that the image coordinates obtained by the digital point determination also for these two targets were sufficiently accurate to be used as initial values for a consequent more precise measurement (see Introduction).
- The inner ellipse (corresponding circle, see fig. 4 a, b) could not be detected in most cases
- Neither could the middle ellipse be distinguished in many cases. The similarity criteria (stated in step 2 of the algorithm described above) had thus to be modified.

Accuracy:

The actual figures are given in table 1. The following comments are noted:

- The difference between *digitally* and *analogly measured image coordinate* also contains the influence of the manual setting error, which was not evaluated by this experiment. When the image is elliptical a lower precision is expected than when it is circular or an orthogonal cross (which may give a standard setting error of 1-2μ). Reducing the mean square difference of dx_c and dy_c by a standard setting error 3μ (0.20 of pixelsize=15μ) would give the following mean square error of one digitally measured coordinat:
  $\sqrt{0.39^2-0.20^2}=0.35$ of the pixelsize.
- A trend towards gettting too large b/a was observed for the smallest values of a and b/a.

Appendix A. How to determine the ellipse orientation κ' from intersecting the ellipse by lines parallel to the x- and y-directions

The distance between two ellipse points defines a chord. Regard two sets of chords parallel to the x- and y-directions respectively (fig. 2). It will be shown that κ' (fig. 1) can be derived from the directions $\Phi_{dia\ i\ (i=1,2)}$ of the two diameters each of which halves one set of chords. The equation for the ellipse can generally be written in polynomial form as:

$$(f=)\quad A x^2 + B x y + C y^2 + D x + E y + F = 0 \qquad (A1a)$$

or

$$(f=)\quad A(x-x_c)^2+B(x-x_c)(y-y_c)+C(y-y_c)^2 + F = 0 \qquad (A1b)$$

Introducing system (x',y') with origin at the ellipse centre and x' parallel to the large axis,

$$(x-x_c) = x' \cos\kappa' - y' \sin\kappa' \qquad (A2)$$
$$(y-y_c) = x' \sin\kappa' + y' \cos\kappa'$$

we can write the ellipse equation in the following forms :

$$A' x'^2 + B' x' y' + C' y'^2 + F' = 0; \qquad B' = 0 \qquad (A3a)$$
$$x'^2/a^2 + y'^2/b^2 - 1 = 0 \qquad (A3b)$$
$$x' = a \cos\alpha,\ y' = b \sin\alpha \qquad (A3c)$$

Some notations used:

α	: parameter interpreted as a target angle projected as α' (fig. 7)
a, b	: semi-major and semi-minor axes, respectively
(x, y)	: original image coordinate system
(x_c, y_c)	: centre of ellipse
κ'	: direction of major axis (with reference to the orginal system)
A, B,..	: coefficients of the polynomial in the sytem (x, y)
A', B',..	: coefficients of the polynomial in the system (x', y')

The following relations are valid:

$$tg2\kappa' = B/(A-C), \qquad (A4a)$$
$$A' = A\cos^2\kappa' + B\cos\kappa'\sin\kappa' + C\sin^2\kappa', \quad C' = A\sin^2\kappa' - B\sin\kappa'\cos\kappa' + C\cos^2\kappa', \quad F' = F \qquad (A4b)$$
$$a^2 = -F'/A', \qquad b^2 = -F'/C', \qquad (b/a)^2 = A'/C' \qquad (A4c)$$

The mentioned directions $\Phi_{dia\ i\ (i=1,2)}$ can be found by fitting two lines

$$y - y_{0_i} = (x - x_{0_i})\ tg\ \Phi_{dia\ i}, \qquad i = 1, 2 \qquad (A5)$$

to midpoints of chords of their respective set. (x_{0_i}, y_{0_i}: shift parameters).

Equation (A6) is also fundametal by which the tanget direction Φ_p in an arbitrary point $P'(x_p,y_p)$ on the ellipse is given. (A6) is obtained by first differentiating equation (A1b)

$$\partial f/\partial x\ dx + \partial f/\partial y\ dy = 0$$

where the derivates df/dx, df/dy become simple expressions in A, B, C, and then setting

$$dx = \sin\Phi_p, \quad dy = \cos\Phi_p, \quad x = x_p, \quad y = y_p$$

The result is:

$$(2A\ (x_p-x_c) + B\ (y_p-y_c))\ \sin\Phi_p + (2C\ (y_p-y_c) + B\ (x_p-x_c))\ \cos\Phi_p = 0 \qquad (A6)$$

From (A6), the two particular equations for the tangents at the ellipse points P'_1 and P'_2, fig. 2, are obtained by substituting index p with p_1 and p_2, respectively. Then introducing :

$$\Phi_{p_1} = \Phi_{dia\ 1}, \quad \Phi_{p_2} = \Phi_{dia\ 2}, \quad x_{p_2}-x_c = y_{p_1}-y_c = 0, \qquad (A7)$$

we get from (A4a)

$$tg\ 2\kappa' = 2/(tg\ \Phi_{dia\ 2} - tg\ \Phi_{dia\ 1})^{-1} \qquad (A8)$$

Appendix B. How to derive exact linear equations expressing a) the co-linearity condition and b) the co-planarity condition

a). The error equations expressing the *co-linearity* condition can be written as (fig. 8)

$$\mathbf{x}_i - m_i \mathbf{R}(\mathbf{X}_i - \mathbf{X}_0) = \mathbf{e}_i \qquad (B1)$$

$$\mathbf{a}^T \mathbf{a} = 2 \qquad (B2)$$

where

$\mathbf{x}_i^T$ = {x, y, z}$_i$: image point P'$_i$ (z_i = -camera constant)
$\mathbf{X}_i^T$ = {X, Y, Z}$_i$: object point P_i
$\mathbf{X}_0^T$ = {X_0, Y_0, Z_0}: projection centre O
$\mathbf{e}_i^T$ = {e_x, e_y, e_z}$_i$: observational errors ($\sigma_x = \sigma_y = \sigma_o$, $\sigma_z = 0$)
$\mathbf{a}^T$ = {a, b, c, d}: Rodrigues parameters
m_i : point scale
R : rotation matrix, the elements of which are dependent on **a** by the identity:

$$\mathbf{R} = (d\,\mathbf{I} - \mathbf{C}^*)^{-1}(d\,\mathbf{I} + \mathbf{C}^*), \quad \mathbf{C}^* = \begin{Bmatrix} o & -c & b \\ c & o & -a \\ -b & a & o \end{Bmatrix}, \quad \mathbf{I} = \text{unit matrix} \qquad (B3)$$

After introducing this expression for **R** into (B1), and reordering, we get error equations with the left-hand side being linear in **a** and $\mathbf{X'}_0$, (considering m_i, $\mathbf{x}_i$ and $\mathbf{X}_i$ as knowns):

$$m_i^{-1}(d\,\mathbf{I} - \mathbf{C}^*)\,\mathbf{x}_i - (d\,\mathbf{I} + \mathbf{C}^*)\,\mathbf{X}_i + \mathbf{X'}_0 = m_i^{-1}(d\,\mathbf{I} - \mathbf{C}^*)\,\mathbf{e}_i \qquad (B4)$$

where

$$\mathbf{X'}_0 = (d\,\mathbf{I} + \mathbf{C}^*)\,\mathbf{X}_0$$

b). For a stereo pair the following equations are *generally* valid (l: left, r: right):

$$(m_i^{-1}\mathbf{R}^T\mathbf{x}_i - \mathbf{X}_i + \mathbf{X}_0 = m_i^{-1}\mathbf{R}^T\mathbf{e}_i)_l$$
$$(m_i^{-1}\mathbf{R}^T\mathbf{x}_i - \mathbf{X}_i + \mathbf{X}_0 = m_i^{-1}\mathbf{R}^T\mathbf{e}_i)_r \qquad (B5)$$

where $\mathbf{X}_i$ are common parameters. After eliminating $\mathbf{X}_i$, and reordering, we obtain the following error equations expressing the *co-planarity* condition:

$$(m_i^{-1}\mathbf{x}_i)_l - (m_i)_r^{-1}\,\mathbf{R'}\,(\mathbf{x}_i)_r + \mathbf{X''}_0 = \mathbf{e'}_i \qquad (B6)$$

where

$$\mathbf{R'} = \mathbf{R}_l\,\mathbf{R}^T_r \quad (=\{r'_{ij}\} = \{\mathbf{r'}_1, \mathbf{r'}_2, \mathbf{r'}_3\}^T)$$
$$\mathbf{X''}_0 = \mathbf{R}_l((\mathbf{X}_0)_l - (\mathbf{X}_0)_r)$$
$$\mathbf{e'}_i = (m_i^{-1}\,\mathbf{e}_i)_l - (m_i^{-1}\,\mathbf{R'}\,\mathbf{e}_i)_r$$

In the *asymmetrical case*, $\mathbf{R}_l = \mathbf{I}$, $(\mathbf{X}_0)_l = \mathbf{0}$ are valid, so that $\mathbf{R'} = \mathbf{R}^T_r$, $\mathbf{X''}_0 = -(\mathbf{X}_0)_r$.
If an expression for **R**, like (B3) is introduced into (B6), the left-hand sides of the resulting equations become linear in $(\mathbf{a}, \mathbf{X'}_0)_r$, (considering $(\mathbf{x}_i, m_i)_l$ and $(\mathbf{x}_i, m_i)_r$ as knowns):

$$(m_i)_l^{-1}\,(d\,\mathbf{I} + \mathbf{C}^*)_r\,(\mathbf{x}_i)_l - (m_i^{-1}\,(d\,\mathbf{I} - \mathbf{C}^*)\,\mathbf{x}_i + \mathbf{X'}_0)_r = (d\,\mathbf{I} + \mathbf{C}^*)_r\,\mathbf{e'}_i \qquad (B7)$$

where

$$(\mathbf{X'}_0 = -(d\,\mathbf{I} + \mathbf{C}^*)\,\mathbf{X}_0)_r$$

Remarks:

- The error expressions on the right-hand sides of (B4) and (B7) are dependent on unknowns The linear solving must, therefore, neglect these expressions and use simplified weighting.
- (B2) constitutes a non linear constraint. The solving can, however, be based on (B1) with **a** replaced by **a'**={a',b',c',d'} and with one element of **a'**, =1. (If e. g. d'=1, then **a'**=**a**/d). (Singularity problems might occur if the corresponding element of **a** is relatively small)

Appendix C. Relations between ellipse parameters, local image affinity and camera orientation

Some notations that will be used:

x, y, z	: image system
X, Y, Z	: object system with X-,Y axes in the object plane under consideration
a, b, κ'	: ellipse parameters (see Appendix A)
α, ν, κ, X_0, Y_0, Z_0	: camera orientation (see Appendix B)
r_{ij} (i,j=1,3)	: elements of camera rotation **R**
$\mathbf{x}_c=\{x_c, y_c, z_c\}$	: centre of a small image area, e. g. an ellipse (z_c=-camera constant)
m_c	: point scale of this centre
r	: radius of target circle
b_{ij} (i=1,2; j=1,3)	: parameters of the local affinity in the image of a plane object area
$\mathbf{X}_c=\{X_c,Y_c,Z_c\}$	: centre of a small plane object area, e. g. a circular target

r_{ij} are related to α, κ and ν as follows (Ackermann and Schwidefsky (1976), p. 27):

$$\begin{Bmatrix} r_{11}, r_{12}, r_{13} \\ r_{21}, r_{22}, r_{23} \\ r_{31}, r_{32}, r_{33} \end{Bmatrix} = \begin{Bmatrix} \cos\alpha\cos\kappa+\sin\alpha\cos\nu\sin\kappa, & -\sin\alpha\cos\kappa+\cos\alpha\cos\nu\sin\kappa, & \sin\nu\sin\kappa \\ -\cos\alpha\sin\kappa+\sin\alpha\cos\nu\cos\kappa, & \sin\alpha\sin\kappa+\cos\alpha\cos\nu\cos\kappa, & \sin\nu\cos\kappa \\ -\sin\alpha\sin\nu, & -\cos\alpha\sin\nu, & \cos\nu \end{Bmatrix} \quad (C1)$$

a How the local affinity parameters b_{ij} are related to the camera orientation

Let us rewrite the equations (B1) with **e=0**, as follows (for convenience index i is dropped):

$$\mathbf{X}-\mathbf{X}_0 = m^{-1}\mathbf{R}^{-1}\,\mathbf{x} \quad (C2)$$

We can now find how the differential coordinates dx,dy with reference to point (x_c,y_c) are related to corresponding target coordinates dX,dY with reference to point (Xc,Yc), by deriving differential equations on the basis of (C2) as follows:

$$\begin{aligned} dX &= (\delta fx/\delta x)_c\, dx + (\delta fx/\delta y)_c\, dy \\ dY &= (\delta fy/\delta x)_c\, dx + (\delta fy/\delta y)_c\, dy \end{aligned} \quad (C3)$$

where fx, fy are the right-hand sides of the two first equations of (C2). With x,y restricted to a small definite area around point (x_c,y_c), the following relations are valid to a good approximation when introducing (dX, dY, dx, dy) = ($X-X_c$, $Y-Y_c$, $x-x_c$, $y-y_c$):

$$\begin{aligned} X-X_c &= b_{11}(x-x_c) + b_{12}(y-y_c) \\ Y-Y_c &= b_{21}(x-x_c) + b_{22}(y-y_c) \end{aligned} \quad (C4)$$

or

$$\begin{aligned} X &= b_{11}x + b_{12}y + b_{13}, \quad \text{with } b_{13} = -b_{11}x_c - b_{12}y_c + X_c \\ Y &= b_{21}x + b_{22}y + b_{23}, \quad \text{with } b_{23} = -b_{21}x_c - b_{22}y_c + Y_c \end{aligned} \quad (C5)$$

where $b_{ij\ (i,j=1,2)}$, the partial derivates in (C3), can be expressed as follows:

$$\left.\begin{aligned} b_{11} &= m_c^{-1}(-r_{13}(X_c-X_0)/(Z_c-Z_0) + r_{11}) = m_c^{-2}(-r_{32}\,y_c/z_c+r_{22})z_c/(Z_c-Z_0) \\ b_{12} &= m_c^{-1}(-r_{23}(X_c-X_0)/(Z_c-Z_0) + r_{21}) = m_c^{-2}(r_{32}\,x_c/z_c-r_{12})z_c/(Z_c-Z_0) \\ b_{21} &= m_c^{-1}(-r_{13}(Y_c-Y_0)/(Z_c-Z_0) + r_{12}) = m_c^{-2}(r_{31}\,y_c/z_c-r_{21})z_c/(Z_c-Z_0) \\ b_{22} &= m_c^{-1}(-r_{23}(Y_c-Y_0)/(Z_c-Z_0) + r_{22}) = m_c^{-2}(-r_{31}x_c/z_c+r_{11})z_c/(Z_c-Z_0) \end{aligned}\right\} \quad (C6a)$$

with

$$m_c = z_c/((X_c-X_0)r_{31}+(Y_c-Y_0)r_{32}+(Z_c-Z_0)r_{33}) = (x_c r_{13}+y_c r_{23}+z_c r_{33})/(Z_c-Z_0) \quad (C6b)$$

Similar expressions are obtained for b_{13} and b_{23} by (C2) (with index c), (C5) and (C6).
$b_{ij\ (i=1..2;\ j=1,3)}$ are thus functions of either $(r_{ij}, X_c-X_0, Y_c-Y_0, Z_c-Z_0, z_c)$
or $(r_{ij}, x_c, y_c, z_c, Z_c-Z_0)$.

b How the ellipse parameters (a,b,κ') are related to the local affinity and target radius

Let us first find how the ellipse parameters A,B,C,F in (A1b) are related to $b_{ij(i,j=1..2)}$ and r. Introducing the expressions (C4) for $X-X_c$ and $Y-Y_c$ into the equation for the circle in the target, a polynomial equation of type (A1) is obtained as follows:

$$(X-X_c)^2+(Y-Y_c)^2-r^2=0 \quad \Leftrightarrow$$
$$(b_{11}^2+b_{21}^2)(x-x_c)^2+(b_{12}^2+b_{22}^2)(y-y_c)^2+2(b_{11}b_{12}+b_{21}b_{22})(x-x_c)(y-y_c)-r^2=0 \qquad (C8)$$

From (C8) and (A1), we see that A,B,C,F are related to $b_{ij\ (i,j=1,2)}$ and r as follows :

$$A = b_{11}^2+b_{21}^2, \qquad B = 2(b_{11}b_{12}+b_{21}b_{22}), \qquad C = b_{12}^2+b_{22}^2, \qquad F=-r^2 \qquad (C9)$$

The required relations are then obtained on the basis of (C9) and (A4).

Remark:
On the basis of the relations found in **a**, the ellipse parameters (and the point scale) can be expressed in terms of the outer orientation parameters. If the κ-rotated coordinates $(x,y)_\kappa$, given by:

$$x_\kappa = x\cos\kappa + y\sin\kappa$$
$$y_\kappa = -x\sin\kappa + y\cos\kappa \qquad (C10)$$

are used, the point scale is generally:

$$m_c = ((y_c/z_c)_\kappa \sin\nu + \cos\nu)\ (z_c)_\kappa/(Z_c-Z_0) \qquad (C11)$$

and for ellipses with $X_c = 0$ (i. e. their centres are lying on the line through N'-M' (fig. 7)) the parameters are :

$$\kappa'(x_{c\kappa}=0) = \kappa \qquad (C12)$$
$$a\ (x_{c\kappa}=0) = r\,m_c \qquad (C13)$$
$$(b/a)\ (x_{c\kappa}=0) = ((y_c/z_c)_\kappa \sin\nu + \cos\nu) = \cos(\varepsilon+\nu)/\cos\varepsilon, \qquad \mathrm{tg}\ \varepsilon = (y_c/z_c)_\kappa \qquad (C14)$$

c How the camera orientation are related to the ellipse parameters and the target radius

The derivation of this relation will be indicated under the assumption that $x_{c\kappa} = 0$ (conf. Remark above). Under this assumption κ, ν and Z_c-Z_0 can be expressed in in terms of $x_c,y_c,z_c,a,b,\kappa',r$ as follows:

- $\kappa = \kappa'$
- ν derived from (C10) and (C14)
- (Z_c-Z_0) derived from the third equation of (C2) with $m_c=a/r$ (see (C13)) and with r_{i3} depending on κ and ν (see (C1)).

Regardless of the actual value of $x_{c\kappa}$, this derivation (with the approximation $x_{c\kappa}=0$) might, nevertheless, give good enough approximate values for a consequent bundle adjustment.

Note that α cannot be derived by circular target. Note also that if the image of a circular target is nearly circular (i. e. ν is nearly 0), the condition for deriving κ is bad.

d How the affinity between two homologous small areas is related to the camera orientations

Let us assume that these areas are images of a plane object area . Thus the tranformation is:

$$x_l = b'_{11}\, x_r + b'_{12}\, y_r + b'_{13}, \qquad \text{with } b'_{13} = -b'_{11}\, x_{c_r} - b'_{12}\, y_{c_r} + x_{c_l}$$
$$y_l = b'_{21}\, x_r + b'_{22}\, y_r + b'_{23}, \qquad \text{with } b'_{23} = -b'_{21}\, x_{c_r} - b'_{22}\, y_{c_r} + y_{c_l} \qquad \text{(C15)}$$

where

$(x,y,z)_l$, $(x,y,z)_r$: conjugate points in left- and right-hand areas, respectively
$(x_c,y_c,z_c)_l$, $(x_c,y_c,z_c)_r$: centres of these areas

We can now show how the b'_{ij}'s are related to the locations of the homologous areas and to the camera orientations with respect to an object system with X-,Y-axes in the object area. The relation can be derived similarly to the derivation in **a** above. Differentiating (B6) gives:

$$\begin{aligned}
&\{(m_c^{-1} - m_c^{-2} x_c r_{31}) \quad dx + (-m_c^{-2} x_c r_{32}) \quad dy\}_l = \\
&\{(m_c^{-1} r'_{11} - m_c^{-2} r'_1 x_c r_{31})\, dx + (m_c^{-1} r'_{12} - m_c^{-2} r'_1 x_c r_{32})\, dy\}_r \\
&\{(-m_c^{-2} y_c r_{31}) \quad dx + (m_c^{-1} - m_c^{-2} y_c r_{32}) \quad dy\}_l = \\
&\{(m_c^{-1} r'_{21} - m_c^{-2} r'_2 x_c r_{31})\, dx + (m_c^{-1} r'_{22} - m_c^{-2} r'_2 x_c r_{32})\, dy\}_r
\end{aligned} \qquad \text{(C16)}$$

Setting $dx=(x-x_c)$ and $dy=(y-y_c)$ and eliminating either y_l or x_l, gives either x_l or y_l expressed in terms of x_r and y_r like (C15). The b'_{ij}'s are related to the 8 expressions (..) in (C16); i. e. the b'_{ij}'s are related to $(x_c,y_c,z_c,r_{ij},Z_c-Z_0)$ when m_c=the right-hand expression of (C6b) is introduced.

Appendix D. Matching an elliptical image with a circular template

It will be shown that this matching involves 5 geometric unknowns. Let us assume that the elliptical pattern consists of a set of n concentric ellipses i, (i=1,2.. n), and that the circular pattern consists of a set of n concentric circles i, (i=1,2.. n), arranged in such a way that ellipse i is the projection of circle i, with parameters:

r_i, X_c, Y_c : parameters of circle i
a_i, b, κ', x_c, y_c : parameters of ellipse i (see Appendix A)

Let's further assume that for each pair (**c**ircle, **e**llipse)$_i$, a pair of mean gray level values $(g^*_{ci},\ g^*_{el})_i$ is "observed". $(g^*_{el})_i$ can be derived as follows:

$$(g^*_{el})_i = \Sigma g_j / n$$

where g_j is gray level value interpolated in a point $(x',y')_j$ in system x',y' (see (A2)), and

$x'_j = a_i \cos \alpha_j$, $\qquad y'_j = b_i \sin \alpha_j$
$\alpha_j = \alpha_{j-1} + \Delta\alpha$, (j = 1,2,.. n), $\qquad \alpha_0 = 0$
$\Delta\alpha$ = specified value, $\qquad n = 2\pi/\Delta\alpha$

Similar formulas for computing $(g^*_{ci})_i$ can be given (with X,Y in stead of x',y', and $a=b=r$). A procedure for a 1-D least squares matching can then be designed on the basis of the following equation, introducing the parameters $t = a_i/b_i$ and $m = a_i/r_i$:

$$g^*_{ci}(r_i, X_c, Y_c) = h_0 + h_1\, g^*_{el}(r_i, m, t, \kappa', x_c, y_c)$$

where

$g^*_{ci}(..), g^*_{el}(..)$: functions for the mean gray level values for **c**ircles and **e**llipses
r_i, X_c, Y_c : known parameters
m, t, κ', x_c, y_c : unknown geometric parameters
h_0, h_1 : unknown zero level shift and brightness scale

The procedure might be worked out along the same lines as described by Ackermann (1984).

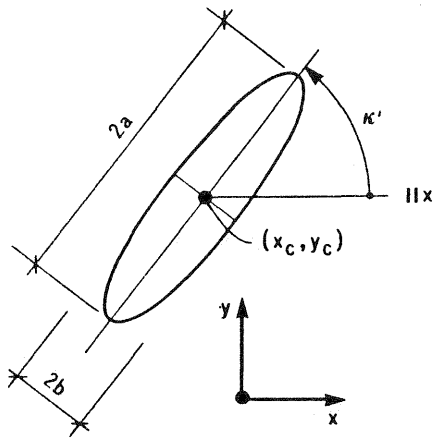

Fig. 1 Shape parameters of the ellipse

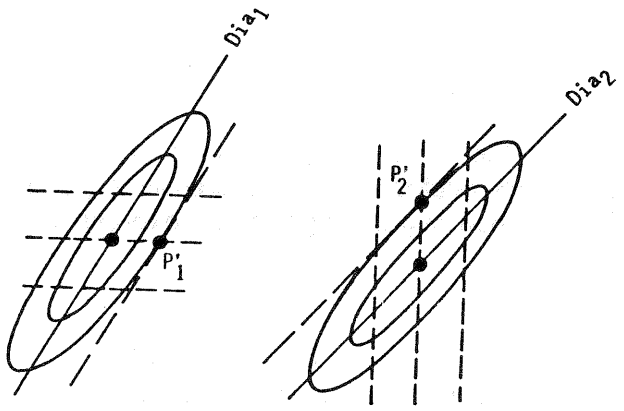

Fig. 2 Intersection lines and diameters

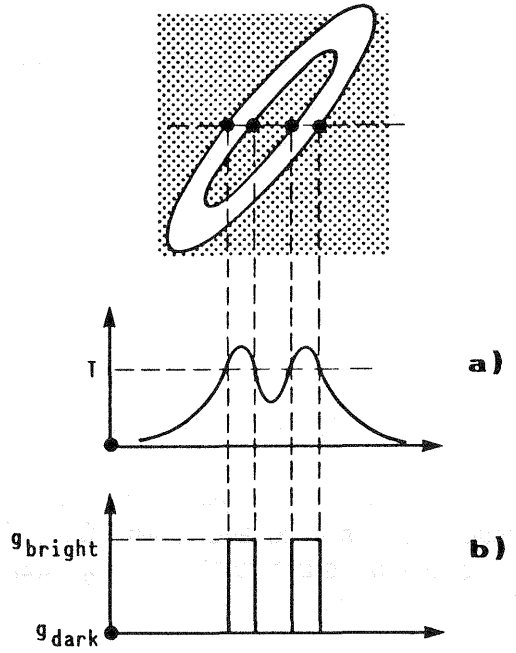

Fig. 3 Gray value distribution of a cross-section before (a) and after (b) segmentation

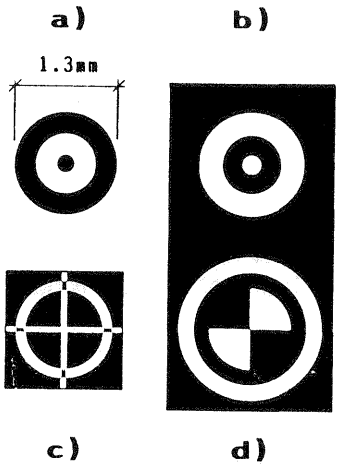

Fig. 4 Types of targets: dark (a) and bright (b) rings, circular-crossed (c), and circular-segmented (d)

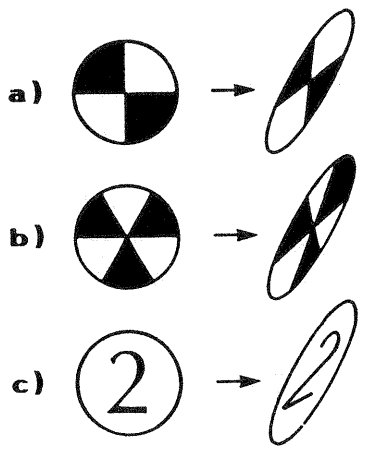

Fig 5. Projections of some targets

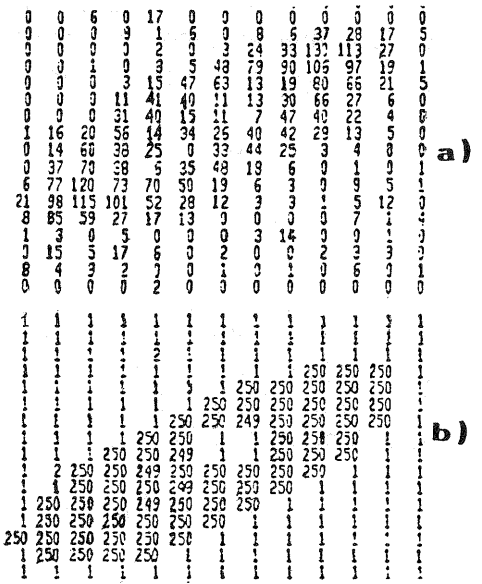

Fig. 6 A window before (a) and after (b) segmentation. Threshold T = 15

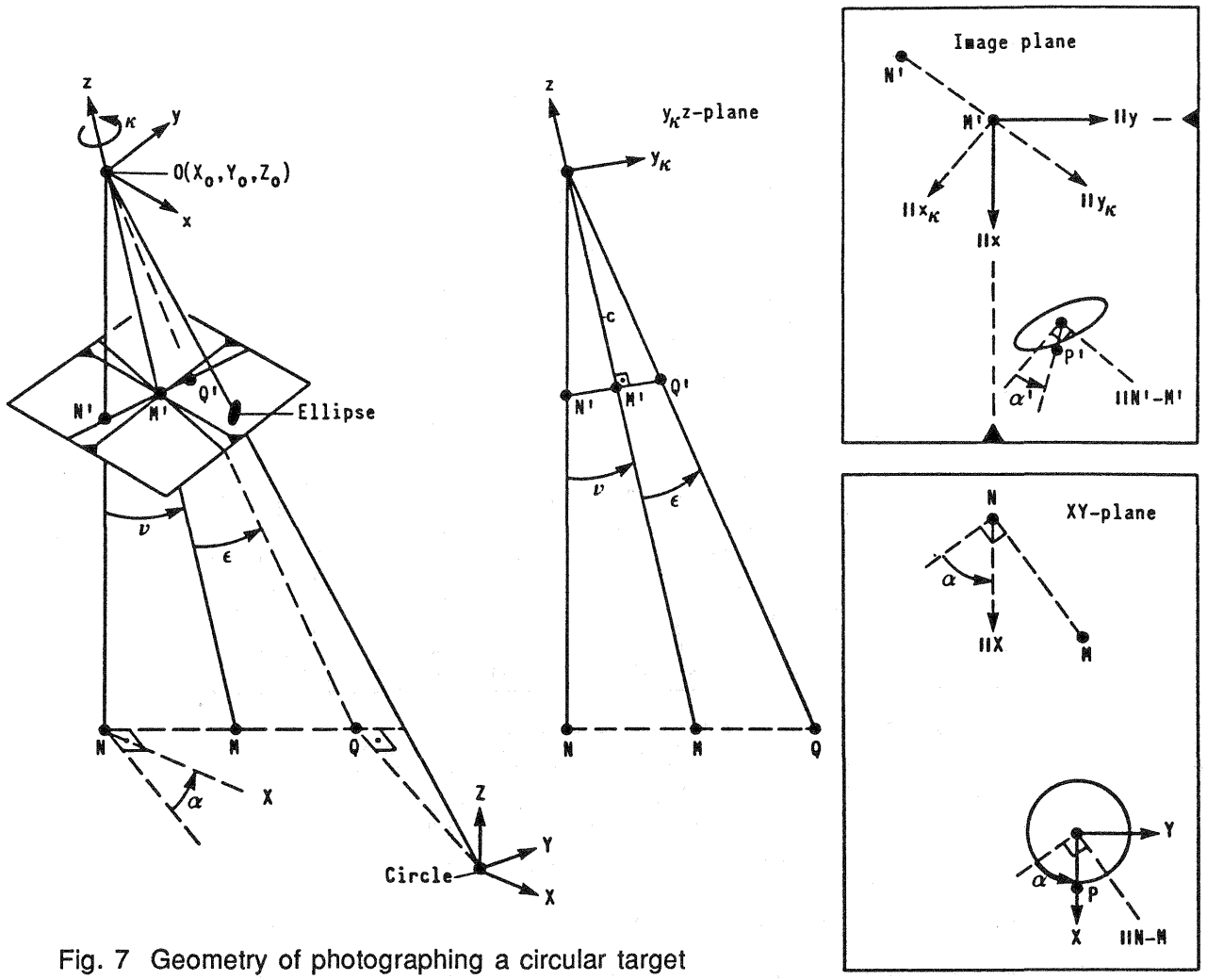

Fig. 7 Geometry of photographing a circular target

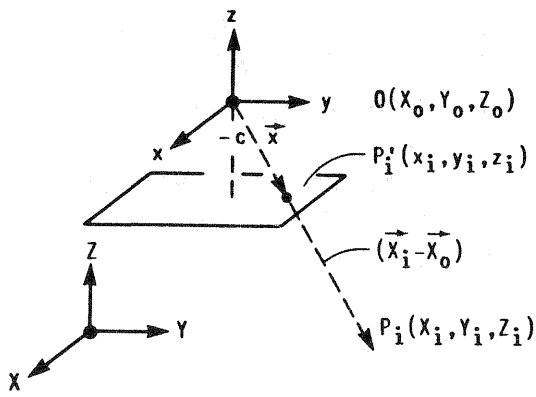

Fig. 8 Co-linearity

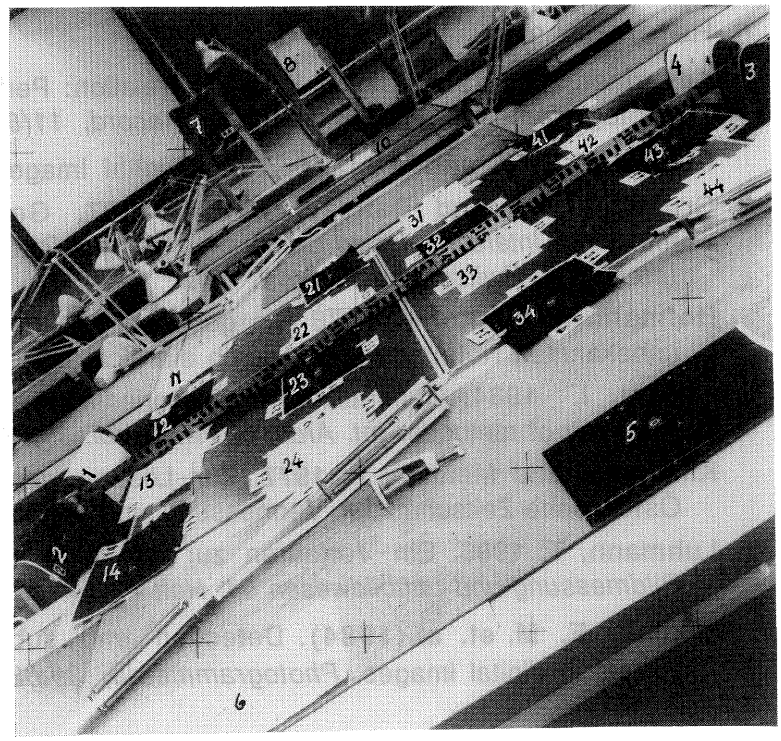

Fig. 9 Photo of the test field

Table 1. RESULT OF THE PRACTICAL EXPERIMENT

Point name	Difference analogly-digitally measured ellipse centre dx µ	dy µ	Digitally derived ellipse parameters (in parenthesis, analytically derived) major axis 2a mm	minor ax./major ax. b/a	ellipse orient-ation κ' 6) g	Point scale 1:	Pixel size µ	Target type (dark or bright ring)
1	-3	5	.30	.47	-53	43	15	dark 2)
2	4	7	.33	.61	-66	36	15	bright 2)
3	8	-2	.46	.48	92	33	30 4)	bright 2)
4	7	7	.35	.37	97	41	15	dark 2)
5	4	-2	.70 (.67)	.49 (.45)	33 (30)	19	30 4)	dark 2)
6	11	-4	.72 (.70)	.47 (.41)	39 (46)	19	30 4)	bright 2)
7	-7	2	.15	.87	5)	93	15	dark 1)
8	-2	3	.15	.73	5)	95	15	bright 1)
9	2	-1	.18 (.17)	.39 (.11)	31 (36)	77	15	dark 1)
11	14	-2	.26 (.26)	.39 (.18)	41 (38)	50	15	dark 1)
12	-5	-5	.32 (.30)	.24 (.20)	43 (39)	43	15	bright 1)
13	28 3)	21 3)	.35 (.36)	.37 (.23)	44 (40)	37	15	dark 2)
14	13	-3	.43 (.46)	.36 (.28)	43 (42)	29	15	bright 2)
21	7	4	.26 (.26)	.39 (.18)	41 (36)	49	15	bright 1)
22	49 3)	0	.30 (.30)	.23 (.21)	37 (37)	43	15	dark 1)
23	-6	-7	.38 (.36)	.34 (.25)	42 (37)	36	15	bright 1)
24	11	3	.44 (.45)	.41 (.31)	42 (39)	29	15	dark 1)
31	-7	11	.26 (.27)	.36 (.18)	44 (35)	49	15	dark 1)
32	-3	11	.32 (.31)	.31 (.21)	39 (35)	42	15	bright 1)
33	-6	7	.36 (.36)	.28 (.25)	34 (34)	36	15	dark 1)
34	10	6	.46 (.46)	.30 (.31)	34 (33)	28	15	bright 1)
41	2	2	.27 (.28)	.27 (.18)	38 (33)	48	15	bright 1)
42	0	2	.29 (.32)	.27 (.20)	36 (33)	41	15	dark 1)
43	-4	0	.36 (.39)	.28 (.23)	33 (31)	34	15	bright 1)
44	6	2	.48 (.50)	.40 (.27)	34 (29)	28	15	dark 2)

1) Only one circle (the outer) was recognized
2) Two circles (the outer and the middle) were recognized
3) Excluded from the computation of mean square difference
4) Every second pixel of 15 µ used
5) The ellipse was too circular to derive its orientation
6) With reference to the fiducial coordinate system

Mean square difference of dx/(pixel size), dy/(pixel size):
0.39 (47 differences)

Mean square difference between digitally and analytically derived a:
4.7 % (19 differences)

Mean square difference between digitally and analytically derived κ' :
4.3 g (19 differences)

Systematic difference between digitally and analytically derived b/a:
28 % (19 differences)

References

Ackermann, F. 1984. Digital image correlation: Performance and potential application in photogrammetry. *Photogrammetric Record, 11(64): 429-439.*

Gonzalez, R. C. and Wintz, P. 1977. Digital Image Processing. *Addison-Wesly*

Gruen, A. W. and Baltsavias, E.P. 1987. Geometrically constrainted multiphoto matching. *Intercommission Conference on Fast Processing of Photogrammetric data. Interlaken, Switzerland, June 2. - 4.*

Hofmann-Wellenhof, B. 1978. Die gegensetige Orientierung von zwei Strahlenbündeln bei unbekannten Nährungswerten durch ein nicht iteratives Verfahren. *Dissertation,TU Graz.*

Hådem, I. 1984. Generalized relative orientation in close range photogrammetry - A survey of methods. *Int. Arch. of Phot., Vol. 35, V, pp. 372-381.*

Killian, K. and Meissel, P. 1977. Zur Lösung geometrisch überbestimmter Probleme. Österrische Zeitschrift für Vermessung und Photogrammetrie, Nr. 3/4, p. 81-.

Luhmann, T. 1986. Ein Verfahren zur rotationinvarianten Punktbestimmung. *Bildmessung und Luftbildwesen 54, Heft 4.*

Mikhail, E. M. et. al.(1984). Detection and sub-pixel location of photogrammetric targets in digital images. *Photogrammetria, 39:63-83.*